Solar-Terrestrial Physics. 2018. Vol. 4. Iss. 4. P. 73–81. DOI: 10.12737/stp-44201810. © 2018 A.G. Sorokin, A.V. Klyuchevskii, V.M. Demyanovich. Published by INFRA-M Academic Publishing House
Original Russian version: A.G. Sorokin, A.V. Klyuchevskii, V.M. Demyanovich, published in Solnechno-zemnaya fizika. 2018. Vol. 4. Iss. 4. P. 95–105. DOI: 10.12737/szf-44201810 © 2018 INFRA-M Academic Publishing House (Nauchno-Izdatelskii Tsentr INFRA-M)

GENERATION OF INFRASONIC SIGNALS DURING EARTHQUAKES UNDER LAKE HOVSGOL (NORTHERN MONGOLIA) ON DECEMBER 5, 2014

A.G. Sorokin
Institute of Solar-Terrestrial Physics SB RAS, Irkutsk, Russia, sor@iszf.irk.ru

A.V. Klyuchevskii
Institute of the Earth's Crust SB RAS, Irkutsk, Russia, akluchev@crust.irk.ru

V.M. Demyanovich
Institute of the Earth's Crust SB RAS, Irkutsk, Russia, vmdem@mail.ru

Abstract. The paper discusses the results of the detection of seismic and infrasonic waves generated by a major earthquake and its aftershock (the moment magnitude M_W=4.9 and M_W=4.2 respectively), which occurred in northern Mongolia under Lake Hovsgol on December 5, 2014. The joint analysis of waveforms of seismic and infrasonic oscillations has shown that the signal recorded by the infrasound station of the Geophysical Observatory of the Institute of Solar-Terrestrial Physics SB RAS (ISTP SB RAS) is formed from sources of three generation types: local, secondary, and epicentral. This analysis enables us to propose a hypothesis of generation of epicentral infrasonic signal by flexural waves in an elastic ice membrane on the surface of Lake Hovsgol, which appear during the passage of seismic wave packets. This hypothesis explains the similarity between seismic and epicentral infrasonic signals, negative initial phase of epicentral infrasonic waves, and detection of a weak signal after a small-magnitude aftershock.

Keywords: aftershock, earthquake, hypocenter, seismic wave, infrasonic wave, flexural wave, epicenter.

INTRODUCTION

One of the sources of infrasonic oscillations is earthquakes: joint seismic and infrasonic signals from severe earthquakes have been recorded for a long time and quite often. The first well-known results of recording of infrasonic signals from earthquakes were related to the recording of vertical oscillations of the earth's surface, generated by transient seismic waves, made by electromagnetic microbarographs at an observation point at the Seismological Laboratory in Pasadena (California, USA) [Benioff, Gutenberg, 1939]. During the Great Alaska Earthquake of March 27, 1964 (magnitude M~9.0), atmospheric pressure waves with an unusually long period (~14 min) were generated. They were clearly detected in Berkeley and at several infrasound stations. The main results were published in a series of articles, which reported on the generation of infrasonic oscillations during vertical movements of the earth's surface, related to local Rayleigh waves [Bolt, 1964; Donn, Posmentier, 1964], as well as with a source in the epicentral region of the Alaska earthquake [Mikumo, 1968]. Later, Young and Greene [1982] identified the third type of generation of infrasonic signals caused by tremors of Rocky Mountains in the North American Cordilleras during the passage of seismic waves from the Alaska earthquake.

The first evidence for the detection of acoustic waves during strong earthquakes in Russia is given by Pasechnik [1959]. The author described infrasonic waves from the disastrous Gobi-Altai earthquake (M=8.1, the intensity in the epicenter I=11÷12), which occurred in the south of Mongolia at a distance of 2440 km from the point of detection on December 04, 1957. The acoustic signal had a long duration (~10 min). This suggests that the emission was remote, long-term, and complex. There was indistinct arrival of the acoustic wave and quasi-sinusoidal shape of the recording. The period of the oscillations at the beginning of the recording was longer than 7–8 s; in the middle, ~4–5 s. The amplitude of the oscillations at the beginning reached 3–4 bar; and in the middle, 5–6 bar. Maximum amplitudes were associated with faulting the earth's surface in the zone of maximum damage caused by the earthquake. It may be noted that the above description of infrasonic oscillations indicates that they originate from sources of three types: local, secondary, and epicentral, as during the Alaska earthquake in 1964.

The scientific interest in acoustic signals from earthquakes is due to at least two factors. First, earthquakes do excite intense acoustic-gravity waves (AGW), as evidenced by the experimental data given above. Second, AGW from powerful ground sources contribute most to the upward energy transfer to ionospheric heights. The structure of AGW occurring during earthquakes is rather complicated and poorly known. Thus, using the Great Alaska earthquake of 1964 as an example, it has been demonstrated that the acoustic signals consist of several wave groups and are generated by successively arriving seismic body longitudinal P-waves and shear S-waves, and then by intense surface Rayleigh waves. Relevant theoretical models of AGW excitation by powerful underground sources were developed later; for example, Rudenko and Uralov [1995] described a physical model of acoustic waves.

Despite the power-law growth of earthquakes with decreasing magnitude, the frequency of detection of infrasonic waves from moderate earthquakes does not

increase, and no infrasonic signals are detected in shocks with M<4 [Arrowsmith et al., 2010]. Perhaps during M<4 earthquakes, seismic vibrations have amplitudes insufficient to generate or record infrasonic waves. It is impossible to detect such vibrations because of the low density of acoustic monitoring networks and conditions of the acoustic signal-to-noise ratio at an observation point. The frequency content of seismic vibrations is quite consistent with the infrasonic range of <20 Hz, even during very weak earthquakes.

EARTHQUAKES AS SOURCES OF INFRASONIC WAVES IN THE BAIKAL REGION

Since 1972 at Badary and Tory stations in the southwest of the Baikal Rift Zone, infrasonic oscillations of different nature have been recorded and studied [Erushchenkov et al., 1979; Sorokin, 1995; Ponomarev et al., 2006; Sorokin, Ponomarev, 2008; Sorokin, Lobycheva, 2011; Sorokin, 2016], but earthquakes as sources of infrasonic signals have not been identified until recently [Sorokin, Dobrynin, 2017]. Figure 1 presents a map of epicenters of 149 earthquakes with magnitude M_{LH}≥4, which occurred in the region from 1972 to 2014 and are a potential source of infrasonic waves. It is seen that the earthquakes happened both in mountainous areas and within rift troughs, and paths of seismic rays to infrasound Badary and Tory stations varied. We have retrospectively reviewed registration books and available records, but the infrasonic signals that were recorded at Badary and Tory stations cannot be unambiguously associated with earthquakes. An exception are two shocks that took place under Lake Hovsgol in the north of Mongolia (the major earthquake of December 05, 2014, 18:04:19.7 UT, φ=51.37° N, λ=100.63° E, the energy class K_p=13.9, the moment magnitude M_W=4.9; aftershock of December 05, 2014, 18:25:09.3 UT, φ=51.36° N, λ=100.65° E, K_p=11.9, M_W= 4.2). During these shocks, at Tory station we identified infrasonic signals closely corresponding to the time at the earthquake source and correlated well with two earthquakes with respect to the time difference between the shocks as well as with respect to magnitudes. This is evidence for the fact of the joint causal effect. The unique character of this pair seismo-acoustic phenomenon suggests an unusual nature of the source of infrasonic signals.

The primary data on the major earthquake and possible source of infrasonic waves are presented in [Sorokin, Dobrynina, 2017]. A further study of factual material relating to the origin of infrasonic signals from the major earthquake has shown that the event is a rather complex phenomenon. This involves particularly the following.

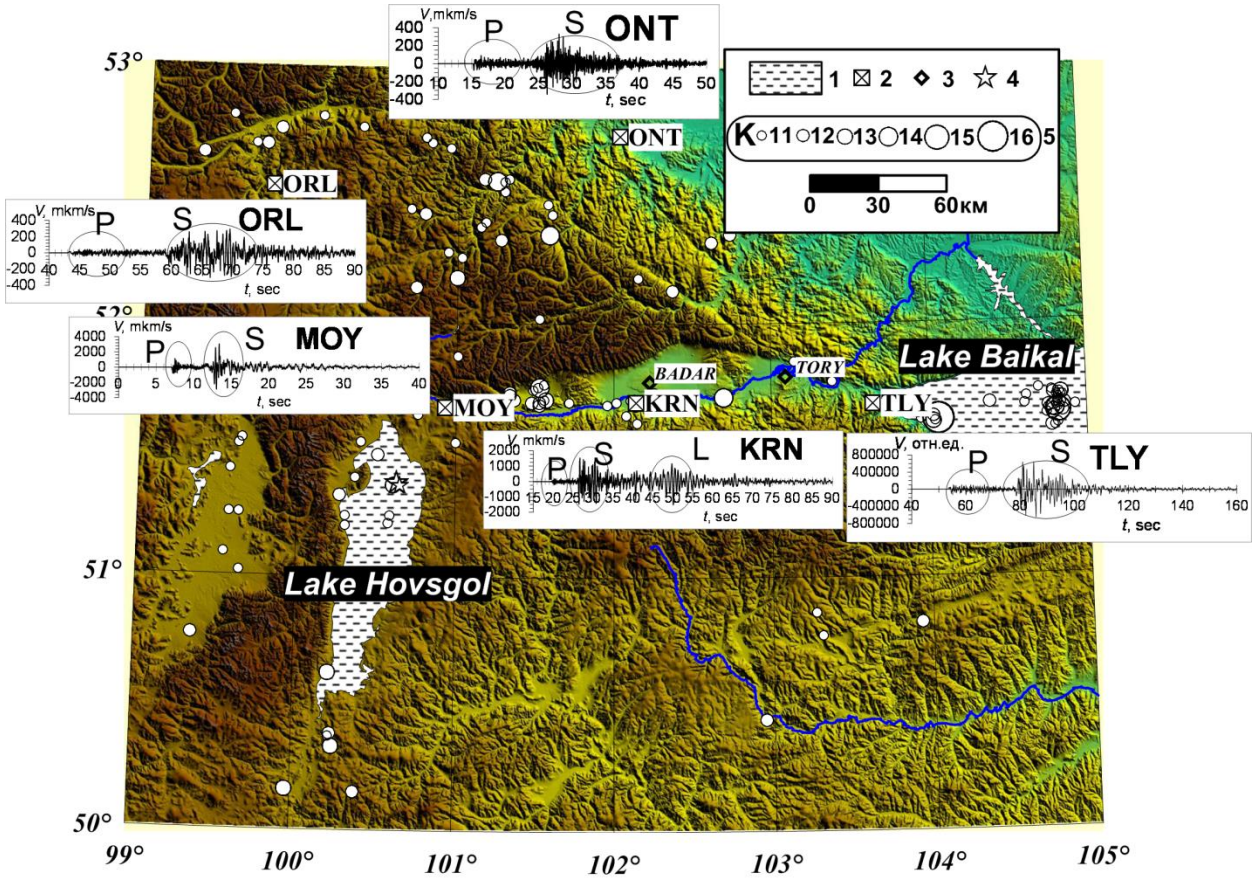

Figure 1. Map of epicenters of severe earthquakes recorded in the southwest of the Baikal Rift Zone from 1972 to 2014: 1 – Lake Hovsgol and Baikal; 2 – seismic stations; 3 – infrasound stations; 4 – epicenters of the major earthquake of December 05, 2014 and its aftershock; 5 – epicenters of earthquakes with K_p≥11. Insets show records of the major earthquake at seismic stations, equipped with broadband instruments Güralp and IRIS. The time in the records of the earthquake is relative

1. The epicentral infrasound has the same form as the seismic signal with pronounced signs of P- and S-waves. This suggests a direct link between the formation of rupture at the earthquake source and excitation of infrasonic signal.

2. The epicentral infrasound has a negative phase of arrival, i.e. it starts with the phase of atmospheric rarefaction. In this case, it is formed due to the downward movement of the surface, which is characteristic of source zones of shocks-faults in the Baikal Rift Zone [Golenetsky, Misharina, 1978; Logatchev, Florensov, 1978].

3. Within 21 min after the major earthquake, an aftershock occurred. Despite the small magnitude, both the seismic events were accompanied by infrasonic signals from a single source, which was likely to have a high Q-factor.

These new facts have not been discussed in previous papers, so they are presented, analyzed, and summarized in this paper.

In the simplest case, to localize the source of infrasonic signals, using data from one observation point, we should know the azimuth of the source, velocity and time of signal propagation in the atmosphere. This approach has been adopted by Dobrynina et al. [2017]; using data on infrasonic oscillation propagation velocity, azimuth and time of arrival of the infrasonic wave from the major earthquake of December 05, 2014 to the station Tory, the authors suggested that the infrasonic signal was generated by a secondary source on the northern slopes of the Khamar-Daban mountain range. As the most probable infrasonic signal generating mechanism, they proposed the interaction of high-amplitude surface seismic waves with mountainous relief of the region. Such an approach to solving the problem about the source of infrasound has not been implemented in [Sorokin, Dobrynina, 2017] because of the lack of accurate time of records of infrasonic signals at Tory station. Here we should note that the timing error between seismic and infrasound data led to incorrect estimation of infrasonic signal propagation time. Hence, the short propagation time provided an opportunity to discover the secondary source of the main phases of infrasonic waves, which did not coincide with the epicenter of the earthquake – it was located approximately at 80 km from the epicenter and emitted through interaction of surface seismic waves with the northwest Khamar-Daban mountain range [Dobrynina et al., 2017]. Unfortunately, for technical reasons the time at Tory station was far behind from accurate global time, so the time of infrasonic signal arrival at the point of detection cannot be used for correct localization of the main source.

To localize the source and to study the nature and mechanism of generation of infrasonic signals from earthquakes of December 05, 2014, we have analyzed waveforms of existing seismic records and the infrasound records we obtained. It has been established that an infrasonic signal is generated by sources of three types: local, secondary, and epicentral. As a source of infrasonic oscillations we take an ice membrane located on the surface of Lake Hovsgol.

ANALYSIS AND INTERPRETATION OF SEISMIC AND INFRASOUND DATA

As is well known [Arrowsmith et al., 2010], infrasonic signals may be generated at an earthquake source and excited by seismic waves transit at secondary sources near observation points for seismic vibrations with amplitudes sufficient to generate infrasonic signals in the dynamic range of recorders. Notice that the generation of infrasonic signals by high-amplitude surface waves at a considerable distance from the earthquake hypocenter reflects the fact of dominance of surface waves over body longitudinal P-waves and shear S-waves for large hypocentral distances when the P- and S-waves are much weaker than the surface waves due to propagation in a volume. Figure 1 shows records of the major earthquake of December 05, 2014 at the seismic stations Mondy (MOY), Orlik (ORL), Kiren (KRN), Onot (ONT), and Talaya (TLY), equipped with Güralp and IRIS broadband instruments. Generally, for such short hypocentral distances records from all the stations clearly exhibit high-amplitude P- and S-wave groups, and low-amplitude surface Love L-waves are observed only at KRN, located in the Tunka valley; a similar picture is seen on aftershock seismograms. Love waves – horizontally polarized SH-waves with low amplitudes that are held near the surface of an elastic body – are formed in a uniform layer lying on a homogeneous half-space with the S-wave velocity greater than the velocity of the waves in the layer [Aki, Richards, 1983]. Such conditions are typical for large rift troughs filled with sediments. Thus, we cannot accept the hypothesis on the interaction of high-amplitude surface seismic waves with mountainous relief of the region as an infrasonic signal generation mechanism [Dobrynina et al., 2017] for the territory of interest: first, there are no surface waves on the records of earthquakes in the mountainous setting of the Tunka valley (MOY, ORL, ONT, TLY); second, the waves are not high-amplitude – they are much weaker than S-waves (KRN). In the data from the On-line Bulletin, International Seismological Centre, acquired by the seismic stations close to the earthquake source, there are no phases of surface waves, they appear for stations located at a greater epicentral distance [http://www.isc.ac.uk].

Figure 2 presents Güralp records of the vertical component HHZ of seismic motion velocity at the seismic station Mondy (MOY) closest to earthquake epicenters. Each of the records shows two wave packets with approximately equal amplitude, but with different frequency content: the first packet at the beginning of a record is a P-wave; the second, an S-wave. The record of the P-wave of the major earthquake has a length $L \approx 1$ s, consists of $n \approx (3 \div 4)$ of smooth oscillations with the maximum amplitude $A \approx 1770$ mkm/s and the frequency $f \approx 3 \div 4$ Hz (Figure 2, *a*). The record of the P-wave of the aftershock $L \approx 1$ s, $n \approx 3 \div 4$, $A \approx 180$ mkm/s, $f \approx 3 \div 4$ Hz (Figure 2, *b*). Approximately 5.5 s after the beginning of the record there appears a body shear S-wave lasting up to 5 s with $A \approx 1850$ mkm/s and $f \approx 1.3$ Hz (Figure 2, *a*); in the aftershock record $A \approx 230$ mkm/s and $f \approx 2$ Hz (Figure 2, *b*).

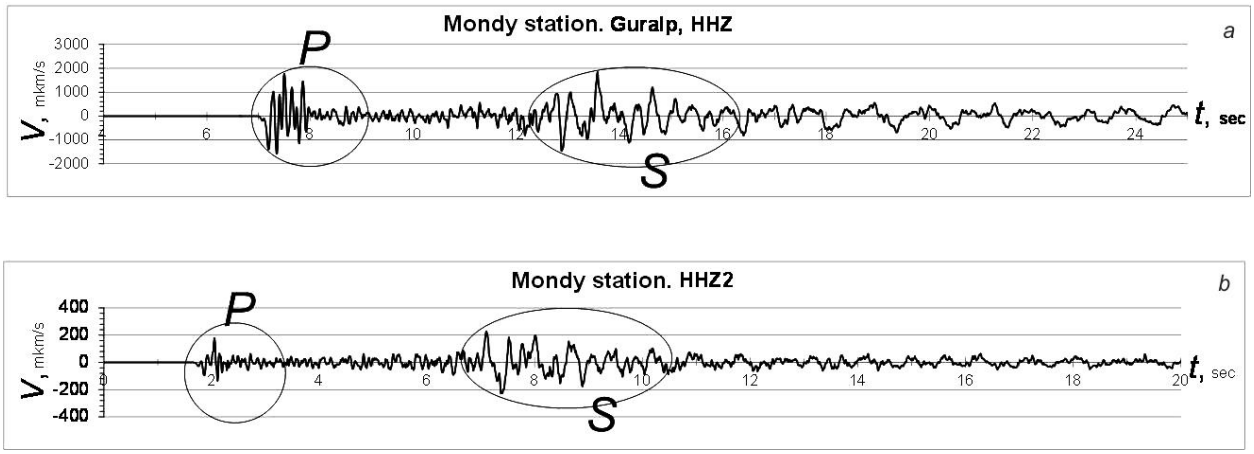

Figure 2. Güralp record of the vertical component HHZ of seismic motion velocity at MOY closest to earthquake epicenters: *a* – the major earthquake, *b* – the aftershock. The former packet at the beginning of the record is a body longitudinal P-wave; the latter, a body shear S-wave. Time is relative

The difference between the arrivals of the P- and S-waves is about 5.5 s, hence the hypocentral distance $r \approx 45$ km (8.1 km/s × 5.5 s≈44.5 km at velocities of the P- and S-waves of 6.4 and 3.58 km/s respectively). The kinematics of the records of the major earthquake and aftershock is virtually repeated, and the amplitude-frequency difference of the records is due to different energy of earthquakes.

The record of infrasonic signals made at the station Tory contains two packets separated in time (Figure 3): the first packet begins as weak oscillations against the background of low-frequency noise, which evolve into high-amplitude oscillations. The second packet, recorded approximately 20 min after the first one, is represented by weak oscillations against the background of low-frequency noise; there are no oscillations with considerable amplitude. The beginning of the record of the former packet corresponds fairly closely to the time at the source of the major earthquake, the time lag between the packets (approximately 20 min) coincides with the time interval between seismic shocks (20 min 50 s), and the level of oscillations in the packets correlates with magnitudes of the major earthquake and aftershock. The azimuth of the infrasonic signal source calculated from the cross-correlation delays between infrasound channels is ~240–270°, thus clearly indicating the earthquake epicenter (Figure 3). All this provides convincing proof of the generation of the infrasonic signals of interest by two earthquakes, which occurred on December 05, 2014 under Lake Hovsgol in northern Mongolia.

The slightly varying signal in the initial part of the record may suggest the arrival of weak infrasonic oscillations with a frequency of ~3 Hz excited by different local and/or secondary infrasound during seismic wave propagation (Figure 4) [Arrowsmith et al., 2010]. It is difficult to identify sources of these oscillations from records of only Tory station: most likely it is the effect of topography. If we associate them with L-waves, then the effect may be attributed to features of bedrock morphology and depth distribution of sediments in Tunka and Tory depressions. Then, in the record we identify the epicentral infrasound [Arrowsmith et al., 2010] – the infrasound generated by vibration of the surface over the earthquake source and beginning with a smooth pulse of considerable amplitude with a frequency of ~1.2 Hz and a duration of <1 s (P). After it for 1 s there are again high-frequency low-amplitude oscillations. Then, for 5 s there is a train of several oscillations with increased amplitude and ~1 Hz frequency (S), after which the infrasound decays and within 1 s there are again high-frequency low-amplitude oscillations. The time difference between the beginning of the first smooth pulse (P) and the train (S) is about 2 s. Then, the record exhibits a group of oscillations with maximum amplitudes with a frequency of <1 Hz and a duration 6–7 s (L). After this group, there is a sharp decrease in the infrasound level and low-level low-frequency oscillations (0.5 Hz) decaying with time. On the background of these low-frequency oscillations there are again the low-amplitude high-frequency oscillations of ~ 3 Hz previously observed at the beginning of the record and at some moments of the infrasound decay. We can take it that the low-amplitude high-frequency oscillations can be seen only when the epicentral infrasound of three wave phases (P, S, L) decreases significantly.

The recording of infrasonic oscillations from a weak aftershock is quite important because it allows us to unambiguously identify a pair of earthquakes as sources of infrasonic signals as well as to explore the possibility of detecting infrasonic oscillations from earthquakes with $M \approx 4$ – the lower limit of magnitudes of the recorded earthquakes generating infrasound [Arrowsmith et al., 2010]. The latter packet of infrasound was recorded within ~21 min after the former and was represented by weak oscillations against the background of low-frequency noise: there are no oscillations with considerable amplitude (Figure 3). We also have a filtered record of infrasonic signals from the aftershock. There are, however, no significant improvements in identification of infrasound; the records exhibit high-frequency oscillations of ~ 3 Hz with minimally resolved amplitude at certain instants. Thus, the latter packet has only weak infrasonic oscillations

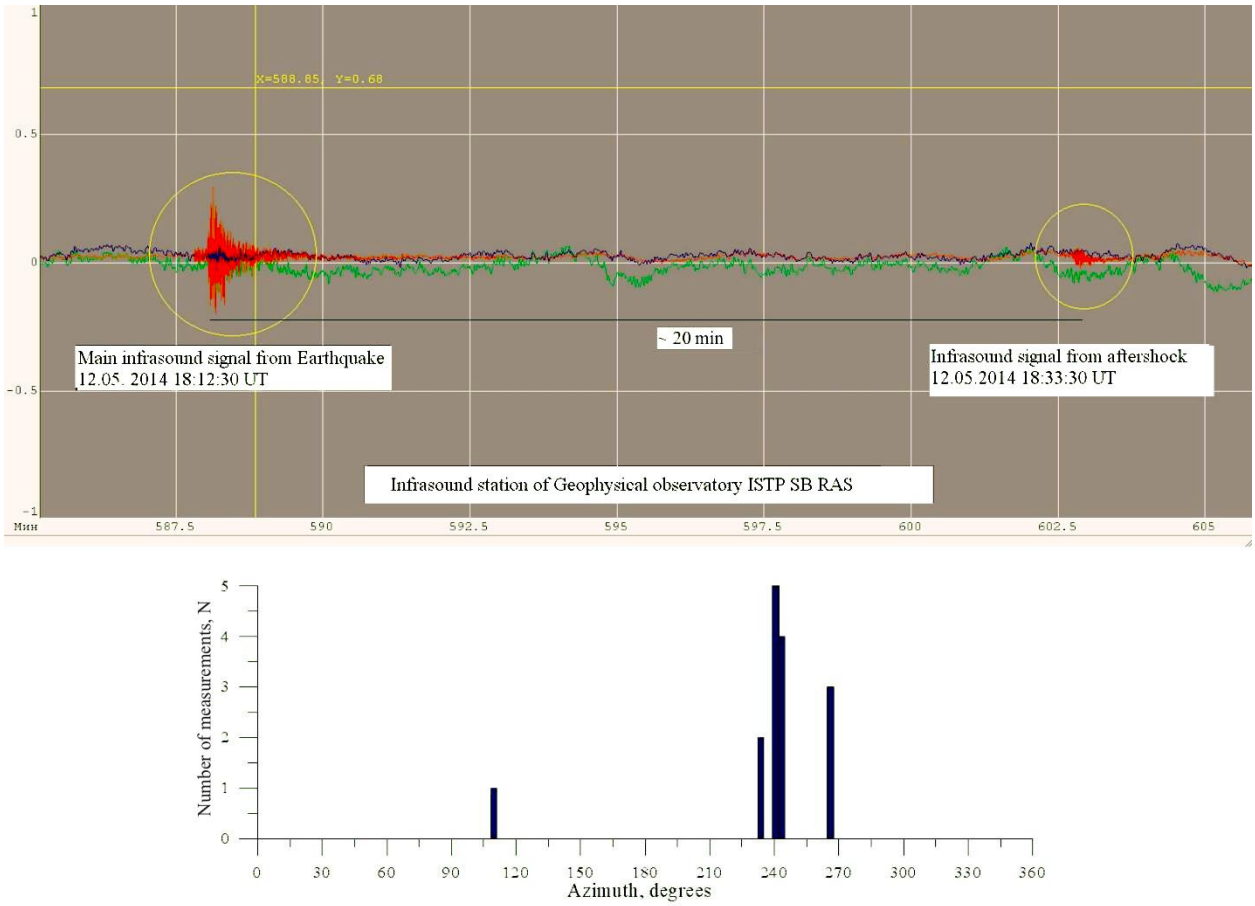

Figure 3. Infrasound response to seismic events (the main shock and aftershock) (top) and azimuths of arrival of infrasound from the major earthquake on December 05, 2014

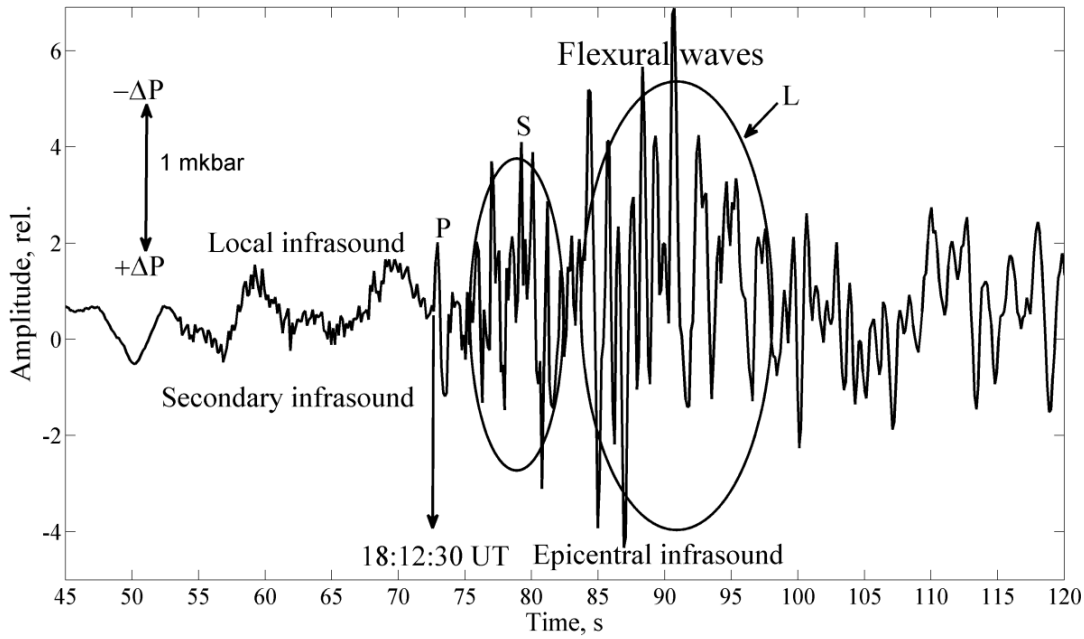

Figure 4. Wave groups in a record of infrasonic oscillations from the major earthquake at Tory station and their interpretation. Intervals of local infrasound, secondary infrasound, and epicentral infrasound (as in [Arrowsmith et al., 2010]) separate the record of infrasonic oscillations into parts according to place and nature of their generation: local (near a recorder during transit of seismic waves), secondary (topography and other features of the earth's crust, such as sedimentary depressions, during seismic wave transit), and epicentral (surface vibrations over the earthquake source), P-, S- and L-signals generated during passage of a body longitudinal P-wave, body shear S-wave, and surface L-wave, and under the formation of flexural waves (infrasound polarity is shown at the top left of the Figure)

with a frequency of ~3 Hz, excited by local and/or secondary infrasound during propagation of seismic waves in a vicinity of Tory station. The epicentral infrasound, which served as the main indicator of infrasound from the major earthquake, was not observed in the aftershock. We assume that if the epicenter of earthquakes is close to Tory station, we can record the epicentral infrasound from the aftershock with $M \approx 4$ and then identify and analyze features of its formation. This example of the record of infrasound from the aftershock with $M \approx 4$ explains how and what limits the recording and identification of infrasonic signals from shocks with $M < 4$. It can be assumed that both in seismology and in acoustics, the main role in the recording is played by the interrelation of earthquake magnitude with the distance between infrasound station and earthquake epicenter: the stronger is an earthquake and the closer is it to the point of recording, the higher is the quality of registogram. Additional conditions such as propagation path, speed limit, direction of infrasound, type of motion at the earthquake source, and features of generation of oscillations by emitting surface are most likely to have secondary importance, but can play a crucial role in detecting local and secondary infrasound.

The joint analysis of waveforms of infrasonic signal and seismogram of the major earthquake allows us to connect the first significant smooth pulse (P) (~1.2 Hz) with the longitudinal P-wave at the earthquake focus when due to the short hypocentral distance the seismic wave has a short pulse duration and is not complicated by inhomogeneities of the medium. We interpret the train of oscillations with increased amplitude (S), a frequency of ~1 Hz, and a duration of ~5 s as a realization of a focal shear S-wave. Since the time difference between the beginning of the first smooth pulse (P) and the train (S) was ~2 s, the infrasound source was at a distance of ~16 km from the earthquake hypocenter (8.1 km/s·2s≈16 km).

Figure 1 indicates that at approximately this distance from the epicenter there are onshore mountain facilities in the west and east of Lake Hovsgol, which can, theoretically, serve as a source of infrasonic waves during high-amplitude seismic oscillations [Le Pichon et al., 2003]. However, the presence of the oscillation group with maximum amplitudes, a frequency of <1 Hz, and a duration 6–7 s in the record allows us to make a more interesting assumption about generation of this group of infrasonic waves by ice surge on Lake Hovsgol due to realization of surface L-waves generated in the sediment layer of the Hovsgol depression. In this case, the smooth pulse and two trains described above are caused by ice surge on the lake under the formation of flexural waves during passage of P-, S- and L-wave packets [Chernykh et al., 2011; 2013]. In these works, the authors have established that body and surface waves from nearby and distant earthquakes can be found in records of ice surges in Lake Baikal. Two variants of propagation of S-wave phases in the ice sheet have been examined: it may be an S-wave propagating from the shore across the ice sheet, and it can be a converted SP-wave appearing on the sediment-water boundary. To identify the seismic waves, their polarization has been determined and compared from the type of waves in rocky soil and ice. The polarization of S-wave records in soil for all shocks had a frequently repeating shape, i.e. it was observed as an ellipse, with the major axis northwestward – southeastward perpendicular to the direction to earthquake epicenters. The S-wave polarization on the ice also had a repeating shape of elongated ellipse with the major axis northeastward – southwestward perpendicular to the preferred orientation of S-wave polarization in soil. The polarization of P-waves in rocky soil and on the ice is virtually the same and coincides with the polarization of S-waves on the ice. Chernykh et al. [2013] have made a preliminary conclusion that there are P- and SP-waves on the ice. This conclusion is confirmed in this work by the fact that during S-wave propagation from the shore across the ice sheet the time difference of the beginning of the first smooth pulse (P) and train (S) should be more than twice as long as 2 s because a seismic signal must reach the shore and then cross the ice. The L-wave might have propagated in a similar way with generation of vertical flexural oscillations of ice under its horizontal shear displacement.

We should consider the distance of 16 km as hypocentral, i.e. as a depth of the hypocenter of the major earthquake, which, according to well-grounded data, is 16.5±4.3 (NEIC) and 22.8 ± 1 km (GCMT) [http://www.isc.ac.uk] In general, the hypothesis of ice surge explains the uniqueness of generation of infrasonic signals from the earthquakes on December 5, 2014 under Lake Hovsgol and the uniqueness of their recording for nearly 150 earthquakes with $M_{LH} \geq 4$ ($M_{LH} \geq 5$ corresponding to the major earthquake with $M_W = 4.9$ was recorded for 17 earthquakes).

MAIN DYNAMIC PARAMETERS OF SEISMIC SOURCES

The above results indicate that seismic vibrations can generate flexural waves in the ice cover of Lake Hovsgol. The set of the established features of infrasound generation by the ice surface of Lake Hovsgol during the December 05, 2014 earthquake is supported by the results of the comparative analysis of records of surface and body seismic waves on the rocky ground and ice of Lake Baikal from the remote East Japan (Tohoku) earthquake (March 11, 2011, at 05 hr 46 min 23 s UTC, $M_W = 9.0$, $\varphi = 38.322°$ N, $\lambda = 142.369°$ E) [Chernykh et al., 2011] and four close weak earthquakes under Lake Baikal [Chernykh et al., 2013]. The generation and resonant amplification of the vertical component of seismic vibrations on the ice sheet are described in detail in these papers without proper analysis of physics of the formation of flexural waves. As derived from [Aki, Richards, 1983], flexural waves refer to the normal mode in an infinite plate, located in vacuum, with motion antisymmetric about the median plane of the plate: an example in nature is waves in floating ice.

Source parameters of the major earthquake and aftershock are determined by D. Brune's model (model of dynamic crack) [Brune, 1970], usually used to find parameters of seismic sources in the Baikal region

[Klyuchevskii, Demyanovich, 2002; Klyuchevskii, 2004; Klyuchevskii, 2008]. The dynamic parameters of earthquake source are calculated from formulas

$$M_0 = 4\pi\rho r V^3 \Phi_0 / \Psi_{\theta\varphi},$$

$$R = 2.34V/(2\pi f_0),$$

$$D = M_0/(\mu S),$$

where M_0 is the seismic moment (dyne·cm), R is the dislocation radius (km), D is the fault slip (mm), ρ=2.7 g/cm^3 is the density of medium, V=3.58 km/s is the velocity of propagation of body shear S-waves, r is the hypocentral distance (km), $\Psi_{\theta\varphi}$=0.6 is the function of direction of vibration from an earthquake source, $\mu=3\cdot10^{11}$ dyne/cm^2 is the shear modulus, S is the fault area (km^2). The calculations have been carried out using data from the Bulletin of the Baikal Branch of the Union Geophysical Survey of the Russian Academy of Sciences [http://www.seis-bykl.ru/]. The calculations have revealed that the mean seismic moment of the major earthquake $M_0 \approx 1.60\cdot10^{17}$ N·m and corresponds to the normal-shear type of movement at the earthquake source. The mean seismic moment of the aftershock $M_0 \approx 1.20\cdot10^{16}$ N·m corresponds to the normal fault. Radii of dislocation of the major earthquake and aftershock vary within $0.67 \le R \le 3.6$ and $0.53 \le R \le 2.8$ km at a mean of $R \approx 2.0$ and $R \approx 1.4$ km respectively. The fault slip during the major earthquake and aftershock varies within $0.17 \le D \le 2.99$ and $0.02 \le D \le 1.56$ m with a mean of $D \approx 1.12$ m and $D \approx 0.26$ m respectively. Note that the mean source parameters agree well with the parameters of strong and moderate earthquakes in the Baikal region [Klyuchevskii, Demyanovich, 2002]. In our studies of the modern geodynamics of the Baikal Rift Zone, Lake Hovsgol is characterized as a structure-attractor of riftogenesis [Klyuchevskii, 2011; Klyuchevskii, 2014]. Such structures determine the current geodynamics and seismogeodynamics of the lithosphere under the evolution of riftogenesis and dynamics of stresses within the bifurcation model with triple equilibrium [Klyuchevskii, 2010]. In these local regions, earthquakes generally occur with normal–fault kinematics of movement; and the December 05, 2014 earthquakes having the kinematics fit well into this model. Notice that the infrasonic signal from the major earthquake has a negative phase of longitudinal wave arrival, reflecting the downward deflection of the ice surface over the focus.

INFRASOUND GENERATION

To describe the generation of infrasound, we adopt the approximation of linear acoustics of an inhomogeneous medium for the wave velocity potential $V=p/(\rho c)$, where p is the pressure purtubation, $\rho=1.29\cdot10^{-3}$ g/cm^3 is the air density, c=320 m/s is the velocity of sound in the atmosphere. Given the velocity of the radiating surface $V \approx Df/r$=0.069 m/s ($D \approx 1.12$ m, f=1 Hz, r=16 km), the amplitude of infrasonic signal over the source is

$$p=\rho cV=1.29\cdot10^{-3}\cdot3.2\cdot10^{3}\cdot6.9\approx28 \text{ dyne/cm}^2 \text{ (μbar)}.$$

This infrasonic signal amplitude is quite detectable by operating instruments and corresponds to amplitudes of the signals previously observed under the MASSA program from large industrial explosions [Alperovich et al., 1983]. The observed signal amplitude is close to the amplitudes of infrasonic signals from seismic sources observed by other authors [Le Pichon et al., 2003, Mutschlecner, Whitaker, 2005], and theoretical estimates of oscillations in the atmosphere associated with seismic movements of the earth's surface [Golytsin, Klyatskin, 1967]. The amplitude of the infrasonic signal of the main shock on December, 05, 2014 in Tory is ~1–2 μbar (Figure 4).

Figure 4 shows a rather complex movement of the emitter, which can be explained by superposition of flexural and seismic waves. We assume that the epicentral infrasound is generated by movements of the ice surface of the lake, formed by the superposition of different modes of flexural waves and seismic wave phases. However, at the initial time, the velocity of the surface is given by a pulse, which is an analog of the pulse of longitudinal P-wave arrival over the source, transformed into a single smooth infrasonic pulse (P) (Figure 4). To construct a possible scenario of pulse formation (P), we employ the solution of the wave equation derived by the finite-difference method for the membrane [Ryndin, Lysenko, 2005]. The calculations employ a 22×22 uniform rectangular coordinate grid for a 4 km rectangular region. Such a size of the region corresponds to the range of radii R of dislocation of the major earthquake. Changes in the main mode of the membrane for a 0.38 s time span with an interval of 0.1 s at a fixed spatial grid for four instants of 0.05, 0.130, 0.255, 0.38 s are shown in Figure 5, *a–d*. There is a well-defined smooth alternating waveform similar to the infrasonic pulse (P). Note that the reported results of generation and emission of infrasonic signals are preliminary and will be refined.

CONCLUSION

The comprehensive analysis of waveforms of seismic and infrasonic oscillations from the December 5, 2014 major earthquake under Lake Hovsgol has shown that the infrasound recorded by the ISTP SB RAS Geophysical Observatory is generated by sources of three types: local, secondary, and epicentral. The high-amplitude epicentral infrasound is generated by the earthquake source due to ice surges on the lake over the earthquake focus under the formation of flexural waves during the passage of packets of longitudinal P-, shear S-, and surface L-waves. Sources of local and secondary low-amplitude infrasonic signals may be numerous and various – they cannot be identified using data from one station. The results give grounds to put forward a hypothesis of generation of epicentral infrasonic signal through superposition of flexural waves of the elastic membrane on the surface of Lake Hovsgol with transient seismic waves. The dynamics and morphology of the main mode of a flexural wave in the first approximation explains the similarity of seismic and epicentral infrasonic signals, negative initial phase of epicentral infrasonic waves, and detection of the weak infrasonic signal appearing after a small-magnitude aftershock. The joint seismo-acoustic study allowed us to refine seismic source parameters and characteristics such as the hypocenter depth, the type of movement at a source, and to identify the generation of surface L-waves in the Hovsgol depression.

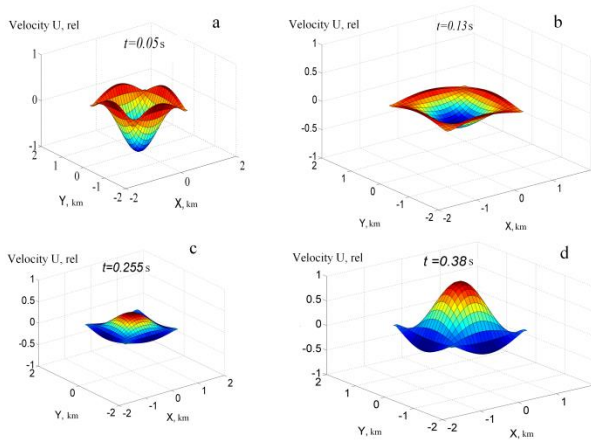

Figure 5. Dynamics and morphology of ice (membranes) surges for the main mode. Seismic P-wave frequency of 1 Hz, seismic emission zone radius ≈2.0 km, times of 0.05 (*a*), 0.130 (*b*), 0.255 (*c*), 0.380 s (*d*)

We are grateful to N.A. Gileva (Baikal Branch of GS FRC RAS) and V.V. Mordvinova (Institute of the Earth's Crust) for kindly providing the records of earthquakes and consultations.

The work was performed with budgetary funding of Basic Research program II.16. The results were obtained using the equipment of the ISTP SB RAS infrasound station.

REFERENCES

Alperovich L.S., Vugmeister B.O., Gokhberg M.B., Drobzhev V.I., Erushchenkov A.I., Ivanov E.A., Kudryavtsev V.P., Kulichkov S.N., Krasnov V.M., Matveev A.K., Mordukhovich M.I., Nagorsky P.M., Ponomarev E.A., Pokhotelov O.A., Tarashchuk Yu.E., Troitskaya V.A., Fedorovich G.V. On experience in modeling magnetospheric-ionospheric effects at seismic events. *Doklady AN SSSR* [Doklady: Earth Sci.]. 1983, vol. 269, no. 3, pp. 573–578. (In Russian).

Aki K, Richards P. *Kolichestvennaya seismologiya* [Quantitative Seismology]. Moscow, Mir Publ., 1983, vol. 1, 2, 880 p. (In Russian).

Arrowsmith S.J., Johnson J.B., Drob D.P., Hedlin M.A.H. The seismoacoustic wavefield: A new paradigm in studying geophysical phenomena. *Rev. Geophys.* 2010, vol. 48, RG4003. DOI: 10.1029/2010RG000335.

Baikalsky Filial FITs EGS RAN [Baikal Branch of Federal Research Center of Geophys. Servey RAS]. http://seis-bykl.ru

Benioff H., Gutenberg B. Observations with electromagnetic microbarographs. *Nature*. 1939, vol. 144, pp. 478. DOI: 10.1038/144478a0.

Bolt B.A. Seismic airwaves from the Great 1946 Alaskan Earthquake. *Nature*. 1964, vol. 202, pp. 1095–1096. DOI: 10.1038/2021095a0.

Brune J.N. Tectonic stress and the spectra of seismic hear waves from earthquakes. *J. Geophys. Res*. 1970, vol. 75, pp. 4997–5009.

Chernykh E.N., Klyuchevskii A.V., Ruzhich V.V. Comparative analysis of recordings of catastrophic East Japan Earthquake on rocky ground and Baikal Lake ice surface. *Voprosy inzhenernoi seismologii* [Problems of Engineering Seismology]. 2011, vol. 38, no. 4, pp. 29–38. (In Russian).

Chernykh E.N., Klyuchevskii A.V., Ruzhich V.V. Comparison of nearby earthquake records on hard rock ground and ice cover of lake Baikal. *Seismic Instruments*. 2013, vol. 49, no.3, pp. 265–274. DOI: 10.3103/S0747923913030067.

Dobrynina A.A., Sankov V.A., Chechelnitsky V.V. Tsydypova L.P., German V.I. Seismic sounding effects from Khuvsgul Lake earthquake of December 5, 2014 with M_w=4.9. *Doklady akademii nauk* [Doklady: Earth Sci.]. 2017. vol. 477, no. 6, pp. 711–715. (In Russian).

Donn W.L., Posmentier E.S. Ground-coupled air waves from the great Alaskan earthquake. *J. Geophys.Res.* 1964, vol. 69, pp. 5357–5361. DOI: 10.1029/JZ069i024p05357.

Erushchenkov A.I., Ponomarev E.A., Sorokin A.G. On microbaroms in East Siberia. *Issledovaniya po geomagnetizmu, aeronomii I fizike Solntsa* [Res. on Geomagnetism, Aeronomy and Solar Physics]. 1979, is. 46, pp. 113–120. (In Russian).

Golenetsky S.I., Misharina L.A. Seismicity and earthquake focal mechanisms in the Baikal rift zone. *Tectonophysics*. 1978, vol. 45, no. 1, pp. 71–86.

Golitsyn G.S., Klyatskin V.I. Atmospheric oscillations caused by movements of Earth's surface. *Izvestiya AN SSSR. Fizika atmosfery i okeana* [Izvestiya: Atmospheric and Oceanic Physics]. 1967, vol. 3, no. 10, pp. 1044–1052. (In Russian).

Klyuchevskii A.V. Seismic moments of earthquakes in the Baikal rift zone as indicators of recent geodynamic processes. *J. Geodynamics*. 2004, vol. 37, no. 2, pp. 155–168.

Klyuchevskii A.V. *Napryazheniya, deformatsii i seismichnost na sovremennom etape evolyutsii litosfery Baikalskoi riftovoi zony* [Stresses, deformations and seismicity at a current stage of evolution of Baikal rift zone lithosphere]. Thesis Dr. Sci. (Geol.-Min). Irkutsk, IEC SB RAS, 2008, 31 p. (In Russian).

Klyuchevskii A.V. Nonlinear geodynamics of the Baikal Rift System: an evolution scenario with triple equilibrium bifurcation. *J. Geodynamics*. 2010, vol. 49, no. 1, pp. 19–23. DOI: 10.1016/j.jog.2009.08.001.

Klyuchevskii A.V. Attractor structure of riftogenesis in the lithosphere of Baikal Rift System. *Doklady: Earth Sci.* 2011, vol. 437, no. 1, pp. 407–411. DOI: 10.1134/S1028334X11030135.

Klyuchevskii A.V. Rifting attractor structures in the Baikal Rift System: Location and effects. *J. Asian Earth Sciences.* 2014, vol. 88, pp. 246–256. DOI: 10.1016/j.jseaes.2014.03.009.

Klyuchevskii A.V., Demjanovich V.M. Source amplitude parameters of strong earthquakes in the Baikal seismic zone. *Izvestiya: Physics of the Solid Earth*. 2002, vol. 38, no. 2, pp. 139–148.

Le Pichon A., Guilbert J., Valle´e M., Dessa J.X., Ulziibat M. Infrasonic imaging of the Kunlun Mountains for the Great 2001 China Earthquake. *Geophys. Res. Let.* 2003, vol. 30, no. 15, pp. 1814. DOI: 10.1029/2003GL017581.

Logatchev N.A., Florensov N.A. The Baikal system of rift valleys. *Tectonophysics*. 1978, vol. 45, pp. 1–13.

Mikumo R. Atmospheric pressure waves and tectonic deformation associated with the Alaskan earthquake of March 28, 1964. *J. Geophys. Res*. 1968, vol. 73, pp. 2009–2025. DOI: 10.1029/JB073i006p02009.

Mutschlecner J.P., Whitaker R.W. Infrasound from earthquakes. *J. Geophys. Res*. 2005, vol. 110, pp. D01108. DOI: 10.1029/2004JD005067.

Pasechnik I.P. Air waves generated during Gobi-Altai Earthquake on December 4, 1957. *Izvestiya AN SSSR. Ser. Geofizicheskaya* [Izvestiya, *Geophysics*]. 1959, no. 11, pp. 1687–1689. (In Russian).

Ponomarev E.A., Rudenko G.V, Sorokin A.G., Dmitrienko I.V., Lobycheva I. Yu. and Baryshnikov A.K. The normal-mode method for probing the infrasonic propagation for purposes of CTBT. *J. Atmosph. Solar-Terr. Phys.* 2006, vol. 68, pp. 559–614.

Rudenko G.V. Uralov A.M. Calculation of ionospheric effects due to acoustic radiation from an underground nuclear explosion. *J. Atmosph. Solar-Terr. Phys*. 1995, vol. 57, no. 3, pp. 225–236.

Ryndin E.A., Lysenko I.E. *Resheniya zadach matematicheskoi fiziki v sisteme Matlab* [Solution of Mathematical Physics Problems with Matlab]. Taganrog, 2005, 65 p. (In Russian).

Sorokin A.G. *Issledovaniya dalnego rasprostraneniya infrazvuka ot vzryvov I okeanskikh shtormov* [Research into long-distance propagation of infrasound from explosions and oceanic storms]. Thesis Cand. Sci. (Phys&Math). ISTP SB RAS, 1995, 10 p. (In Russian).

Sorokin A.G, Ponomarev E.A. Assessing the state of the atmospheric acoustic channel using the IDEAS data on long-distance microbarom propagation. *J. Atmosph. Solar-Terr. Phys*. 2008, vol. 70, pp. 1110–1121.

Sorokin A.G., Lobycheva I. Yu. On simulation of the atmospheric acoustic channel for some nuclear tests in former soviet test site Semipalatinsk. *J. Atmosph. Solar-Terr. Phys*. 2011, vol. 73, pp. 1629–1635.

Sorokin A.G. On infrasonic radiation of Chelyabinsk meteoroid. *Izvestiya RAN. Ser. fizicheskaya* [Izvestiya, *Physics*]. 2016, vol. 80, no. 1. pp. 102–106. (In Russian).

Sorokin A.G., Dobrynina A.A. Comparative analysis of seismic and infrasonic signals from impulse sources and earthquakes. *Izvestiya Irkutskogo gosudarstvennogo universiteta. Ser. Nauki o Zemle* [The Bulletin of Irkutsk State University. Ser. Earth Sci.]. 2017. vol. 20, pp. 107–114. (In Russian).

Young J.M., Greene G.E. Anomalous infrasound generate by the Alaskan earthquake of March 1964. *J. Acoust. Soc. Am.* 1982, vol. 71, pp. 334–339. DOI: 10.1121/1.387457.

URL: http://www.isc.ac.uk (accessed 16.10.2018)

How to cite this article

Sorokin A.G., Klyuchevskii A.V., Demyanovich V.M. Generation of infrasonic signals during earthquakes under Lake Hovsgol (northern Mongolia) on December 5, 2014. *Solar-Terrestrial Physics*. 2018. Vol. 4. Iss. 4. P. 73–81. DOI: 10.12737/stp-44201810.